

This article was downloaded by:

On: 25 January 2011

Access details: *Access Details: Free Access*

Publisher *Taylor & Francis*

Informa Ltd Registered in England and Wales Registered Number: 1072954 Registered office: Mortimer House, 37-41 Mortimer Street, London W1T 3JH, UK



Separation Science and Technology

Publication details, including instructions for authors and subscription information:

<http://www.informaworld.com/smpp/title~content=t713708471>

Design and Simulation of a Microfluidic Blood-Plasma Separation Chip Using Microchannel Structures

Ching-Te Huang^a; Po-Ni Li^a; Ching-Yi Pai^b; Tzong-Shyng Leu^b; Chun-Ping Jen^a

^a Department of Mechanical Engineering, National Chung Cheng University, Chia-Yi, Taiwan, R.O.C. ^b

Department of Aeronautics and Astronautics, National Cheng Kung University, Tainan, Taiwan, R.O.C.

Online publication date: 07 January 2010

To cite this Article Huang, Ching-Te , Li, Po-Ni , Pai, Ching-Yi , Leu, Tzong-Shyng and Jen, Chun-Ping(2010) 'Design and Simulation of a Microfluidic Blood-Plasma Separation Chip Using Microchannel Structures', *Separation Science and Technology*, 45: 1, 42 — 49

To link to this Article: DOI: [10.1080/01496390903402125](https://doi.org/10.1080/01496390903402125)

URL: <http://dx.doi.org/10.1080/01496390903402125>

PLEASE SCROLL DOWN FOR ARTICLE

Full terms and conditions of use: <http://www.informaworld.com/terms-and-conditions-of-access.pdf>

This article may be used for research, teaching and private study purposes. Any substantial or systematic reproduction, re-distribution, re-selling, loan or sub-licensing, systematic supply or distribution in any form to anyone is expressly forbidden.

The publisher does not give any warranty express or implied or make any representation that the contents will be complete or accurate or up to date. The accuracy of any instructions, formulae and drug doses should be independently verified with primary sources. The publisher shall not be liable for any loss, actions, claims, proceedings, demand or costs or damages whatsoever or howsoever caused arising directly or indirectly in connection with or arising out of the use of this material.

Design and Simulation of a Microfluidic Blood-Plasma Separation Chip Using Microchannel Structures

Ching-Te Huang,¹ Po-Ni Li,¹ Ching-Yi Pai,² Tzong-Shyng Leu,² and Chun-Ping Jen¹

¹Department of Mechanical Engineering, National Chung Cheng University, Chia-Yi, Taiwan, R.O.C.

²Department of Aeronautics and Astronautics, National Cheng Kung University, Tainan, Taiwan, R.O.C.

Current clinical methods for the separation of whole blood into blood cells and cell-free plasma are currently based on large facility equipment, such as centrifuges. The disadvantage of this process is that the patients must have assays performed at the hospital or laboratory where the separation facility is located. The present study presents a design for microfluidic chips with different microchannel structures, which utilizes backward facing step geometry and centrifugal force to extract the cell-free plasma from whole blood samples at the branch of the microchannel for further assay, avoiding the influence of blood cells. Numerical simulation was performed on a personal computer to analyze the effects of inlet velocity and the structures of the microchannel on the flow field and back-flow in the microchannel, as well as the efficiency of separation and the volumetric fraction of the flowrate of plasma extraction. The minimum radius of particles (R) that can be excluded from the side channel, and fraction of the volumetric flowrate were obtained to evaluate the efficiency of plasma extraction. Based on the numerical simulations, the design with both converging and bending channels was the best design among the four layouts proposed. In this design, the value of R could be set to less than the critical value (set as 1 μm because of the radius of platelets), and the volumetric fraction of the extraction flowrate was approximately 8.4% when Re was about 20. The preliminary experiments indicated the fluorescent particles with 2.5 μm in radius were successfully excluded from side (plasma outlet) channel of the microfluidic chip with converging a inlet channel and the bent microchannel, when the Reynolds number of the inlet flowrate equals 50.

Keywords backward facing step; microfluidic chips; plasma-skimming; whole blood

INTRODUCTION

Plasma and blood cells are the two major components of whole human blood. In terms of cellular fraction, there

are approximately 5×10^6 cells per microliter of blood, including erythrocytes, leukocytes, platelets, and phagocyte cells (1). Plasma represents nearly 55% of the total blood volume, and this liquid portion of blood is a complex solution containing more than 90% water (2). A heterogeneous group of proteins, mainly composed of albumin, globulins, and fibrinogen, is the major solute of plasma. The relative proportions of plasma proteins will change due to certain diseases, and monitoring such variations could be an effective diagnostic tool. Other ingredients in plasma include salts; glucose; amino acids; vitamins; hormones, such as cortisol and thyroxine; and metabolic waste products, such as urea, uric acid creatinine from the kidneys, and bilirubin from the gall bladder. The constituents in plasma are important in regulating cell function and maintaining homeostasis. For example, potassium affects cell excitability and severe depletion will cause muscle weakness and abnormalities of the cardiac impulse (3). To avoid the protein confounding effects of the cellular fractions of the blood on clinical biochemistry tests (1), the tests are often performed on cell-free samples, such as plasma or serum. Therefore, the separation of plasma and blood cells, so-called plasmapheresis (4), needs to be achieved effectively. Conventionally, a sample of whole blood is sent to a central laboratory, separated by benchtop centrifugation and analyzed sequentially.

As a result of the demand for high efficiency, compact, low-cost, and easy-to-use clinical diagnostics, the application of microfluidics, or miniaturized lab-on-a-chip devices, the development of which has burgeoned in the past decade, has been considered for Point-of-Care (POC) applications (5,6). Conceptually, microfluidic chips are designed to replace classic benchtop centrifugation, as plasma is extracted from whole blood on-chip. The size-exclusion effect, i.e., filtration, resulting from the microstructures in the microfluidic devices, is used to retard cell movement, thereby allowing the collection of the liquid portion of the sample. The filter structures described

Received 25 February 2009; accepted 31 August 2009.

Address correspondence to Chun-Ping Jen, Department of Mechanical Engineering, National Chung Cheng University, No. 168, University Rd., Min-Hsiung, Chia-Yi, 62102, Taiwan, R.O.C. Tel.: +886-5-272-0411, ext: 33322; Fax: + 886-5-272-0589. E-mail: imecpj@ccu.edu.tw

in the literature included comb-type, weir-type, and membrane-type, among others (7–16). The gap or pore size required to achieve retention of erythrocytes is on the order of $1\text{ }\mu\text{m}$ (17), and consequently poses a manufacturing challenge. However, recent reports indicate that high separation efficiency was realized by the filter structures. An integrated microfluidic system, which enables on-chip blood separation and rapid measurement of a panel of plasma proteins from quantities of whole blood within 10 min of sample collection, was investigated (18). A microchip with an interchannel microstructure was employed to separate plasma from human whole blood and to meter the plasma simultaneously in three minutes (19). In the central laboratory, the most frequently used tool is the centrifuge. To miniaturize the centrifuge separation process, centrifugal pumping is employed in the microfluidic chip to transfer different components in the biological sample toward specifically designed regions. Basically, the compact disk (CD)-like platform (20–24) integrates a disposable disk, containing manifolds with microfluidic functions, and a permanent motor plate to provide centrifugal pumping through spinning. However, the simplest approach is to design microfluidic channels for separating blood cells from plasma (17,25–27). The hydrodynamic mechanisms employed in these microfluidic chips are usually the bifurcation law, or plasma-skimming effect (28,29), and the centrifugal force induced by microchannel design.

The present study proposed a design of microfluidic chips for extracting cell-free plasma from a sample of whole blood based on the concept of hydrodynamic filtration (30). The backward facing step structure is designed to enhance the efficiency of cell-free plasma extraction. Four microfluidic channel structure designs are investigated numerically. Simulations using CFD-ACETM (ESI CFD, Inc., France) are performed on a personal computer. The finite element method and three-dimensional structured grids are employed to calculate the pressure and velocity fields in the microfluidic blood-plasma separation chip to evaluate the effects of the structures in extracting cell-free plasma.

PHYSICAL MODEL AND DESIGN OF MICROFLUIDIC CHANNELS

Lateral migration of blood cells takes place in blood flow with low Reynolds number; therefore, a plasma layer adjacent to the channel wall is observed as a result of the so-called plasma-skimming effect. However, the thickness of the cell-free layer is too insignificant to extract cell-free plasma from the whole blood sample (27). The structure of bifurcation was, therefore, employed to separate plasma and blood cells in the present study. When blood cells flow through a bifurcating region of a blood vessel, the cells tend to flow into the daughter vessel with a higher flow rate. This is the so-called Zweifach–Fung effect (bifurcation law). The backward facing step structure was

designed to enhance the efficiency of separation. Flow over a backward facing step would produce pressure loss on the step edge, resulting in characteristics such as reattachment, recirculation, development of shear layers, and separated flows. The structure could induce vortex and turbulence effects in the recirculation region or along the separating shear layer. The inertia of the particles is expected to keep the particles within the recirculation region of the main channel after the branch point and therefore, the particles that enter the side channel would be diminished.

The basic principle of this system is illustrated in Fig. 1. The inlet flowrate is Q_0 , the flowrate of the side channel is Q_1 , and that of the main channel is Q_2 . The dash lines represent the virtual boundaries of flow distributed into side and main channels. The distributed flowrate into the side channel (Q_1) could contain none, small, or large particles, as illustrated in Fig. 1. Assuming the velocity fields follow Poiseuille's Law, the volumetric flowrate ratio of flow into the side and main channel can be expressed as $s_1: s_2 = Q_1: Q_2 = \alpha : (1 - \alpha)$, where α is the ratio of the flowrate in the side channel (Q_1) and inlet flowrate (Q_0). The virtual boundaries (dashed lines) obtained by the simulated streamlines, which extended from the edge of the plasma outlet to the inlet, were used to determine the minimum radius (R) of particles that can be excluded from the side channel, and the fraction of the volumetric flowrate (α). Smaller values of R mean that smaller particles can be filtered by the microchannel. Higher values of α imply a higher efficiency of plasma extraction.

Figure 2 depicted the layouts of the four proposed designs for the microchannel structure. Type I and II are designs with inlet channels of uniform width; type III and IV are those with converging inlet channels. The bent microchannel was employed in Type II and IV to induce centrifugal force. The main channel inlet width is $100\text{ }\mu\text{m}$, the side channel width is $40\text{ }\mu\text{m}$, and outlet width is $204\text{ }\mu\text{m}$. The diameter of leukocytes, which is the largest cell in the blood sample, is about 6 to $10\text{ }\mu\text{m}$; therefore, the feature size of the microchannel must be greater than at least five-fold of the diameter of blood cells to avoid cell attachment at the channel surface in clinical applications. The minimum feature size and the channel height were set for $40\text{ }\mu\text{m}$ in this study. The bent microchannel was employed to generate the centrifugal force, which is expected to enhance the effect of separation. The present design is proposed to miniaturize the centrifuge separation process in the microfluidic channels, instead of the usage of the CD-like platform. The radius of curvature for the bending microchannel in Type II and IV is $455\text{ }\mu\text{m}$, with channel lengths of 2.857 mm , equal to that of Type I and III, and uniform inlet channel widths of $50\text{ }\mu\text{m}$. The centrifugal force could be evaluated as $F = mV^2/r$, where m is the mass of the cells, V is the value of the velocity along the circumference, and r is the radius of curvature for the bending channel. The

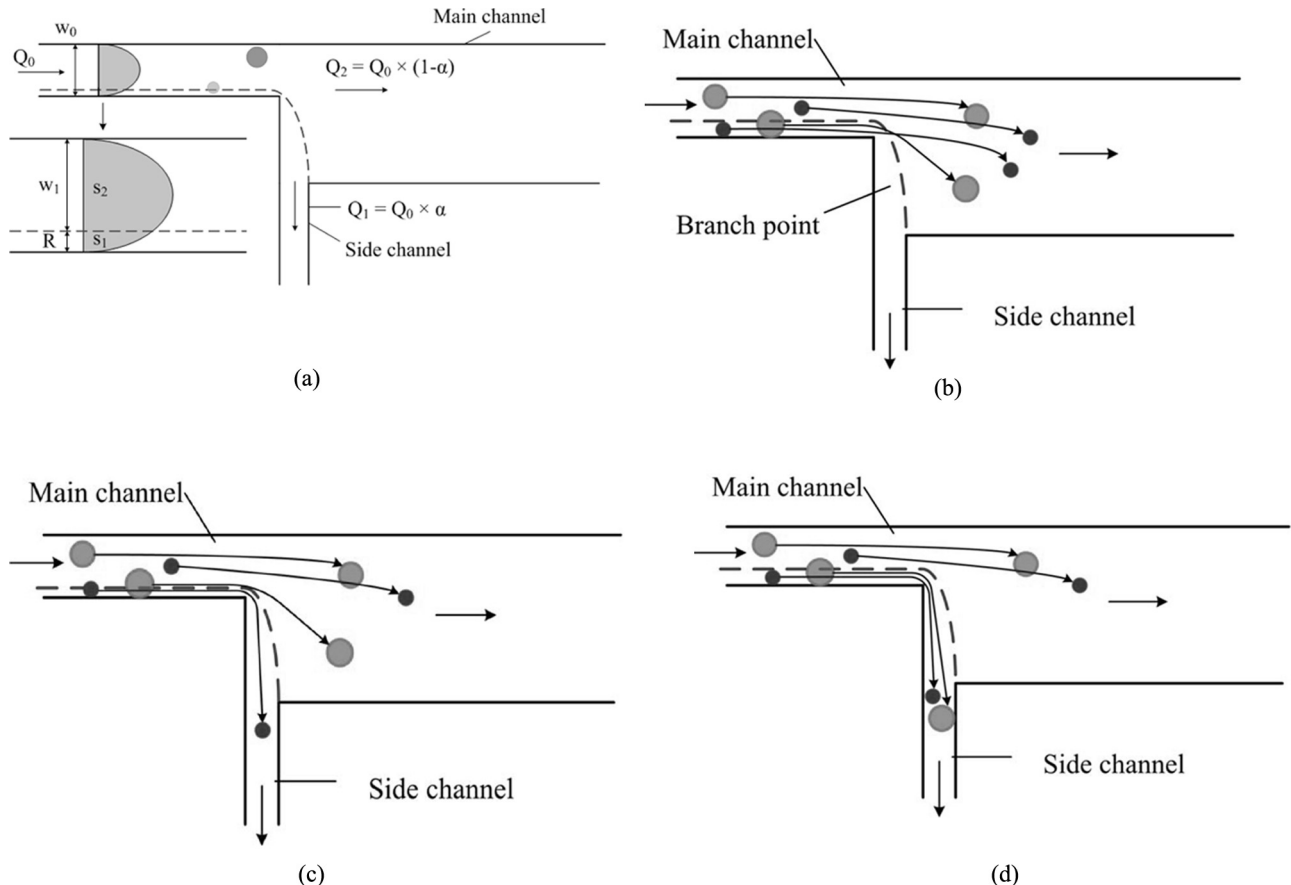


FIG. 1. (a) Schematic illustration of the principle of cell-free plasma extraction from whole blood. The distributed flowrate into the side channel (Q_1) contains (b) no, (c) small or (d) large particles. The dash lines represent the virtual boundaries of the flow distributed into the side and main channels, and are used to determine the minimum radius (R) of particles which can be excluded from the side channel and fraction of the volumetric flowrate (α).

value of the mass of red blood cells is about 34.8 pg (31); therefore, the centrifugal force is calculated approximately 7 pN when the inlet velocity is 0.3 m/s ($Re = 20$).

NUMERICAL SIMULATIONS

Simulations were performed using CFD-ACETM (ESI Group Inc., France) software running on a personal computer. The finite element method and two-dimensional structured grids were employed to solve the governing equations. The governing equations in this study are the continuity and momentum conservation (Navier-Stokes) equations. The dimensionless forms can be expressed as the following:

$$\nabla^* V^* = 0 \quad (1)$$

$$\frac{dV^*}{dt^*} = -\nabla^* P^* + \frac{1}{Re} \nabla^{*2} V^* \quad (2)$$

$$Re = \frac{\rho U D_h}{\mu} \quad (3)$$

D_h and U are the hydraulic diameter of the microchannel and inlet velocity of the fluid, respectively. Laminar flow and adiabatic boundary conditions were set in this simulation. Compressibility and the heating effect in the microchannel were negligible. The SIMPLEC method was adopted for pressure-velocity coupling and all spatial discretizations were performed using the first-order upwind scheme. The simulation was implemented in steady state. A fixed-velocity condition was set as the boundary condition at the inlet of the microchannels, and the outlets were set at a fixed pressure. The whole blood is a suspension of mostly elastic particles (i.e., cells) in a Newtonian fluid of plasma, which results in non-Newtonian characteristics. The viscosity and viscoelasticity of whole blood are dependent on the shear rate of the blood experiences. Furthermore, the whole blood is usually treated by adding some anticoagulant, such as EDTA, or diluted by physiological sodium chloride irrigation solution, whose fluidic properties are similar to water. To simplify the simulation in the present study; therefore, the density and viscosity of blood-plasma were assumed to be the same as water, which are 997 kg/m^3

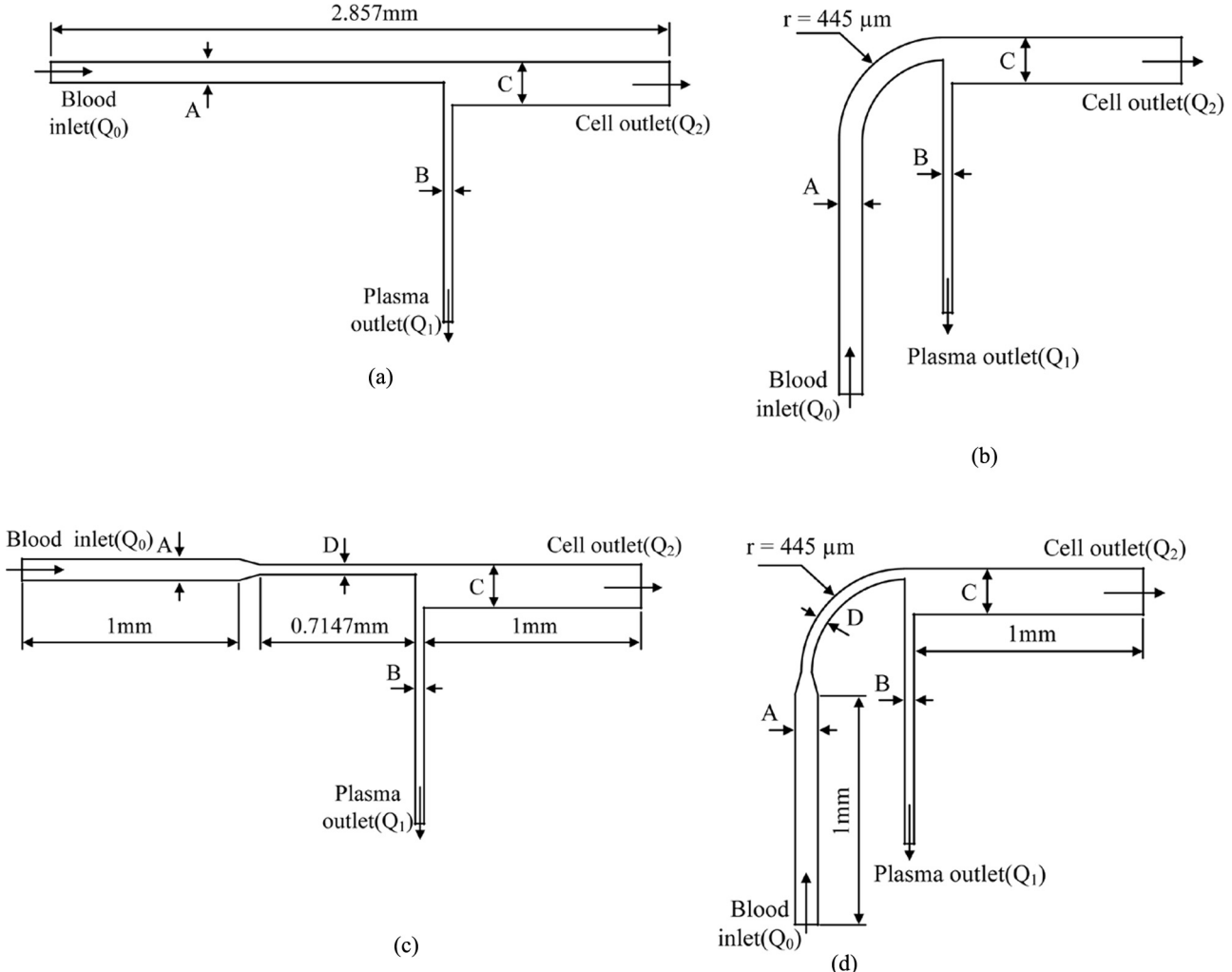


FIG. 2. Layouts of the four proposed microchannel structure designs: Type I (a) and II (b) have inlet channels of uniform width; Type III (c) and IV (d) have constricted inlet channels. The bent microchannel was employed in Type II and IV to induce a centrifugal force ($A = 100 \mu\text{m}$; $B = 40 \mu\text{m}$; $C = 204 \mu\text{m}$; $D = 50 \mu\text{m}$; depth of the microchannel is $40 \mu\text{m}$).

and $8.55 \times 10^{-4} \text{ kg/m-s}$, respectively. The total number of elements was approximately 760,000 in the case of the microchannels.

RESULTS AND DISCUSSIONS

Four microchannel structure designs were investigated in the present work. Type I was the typical backward facing step structure and a bent microchannel was included to induce centrifugal force in Type II. The converging channels in Types III and IV were used to increase the flow velocity at the branch point. The Reynolds numbers of the inlet flowrate in the simulations were set from 50 to 100, which were equal to the flowrate of 18 to $360 \mu\text{L/min}$ (the flowrates could be provided by a commercial syringe pump in practice). The minimum radii (R) of particles which can be excluded from the side channel and the

fractions of the volumetric flowrate (α) obtained by three-dimensional simulations for the different designs, when the Reynolds number equals 5, were shown in Fig. 3. The results indicated that Type III and IV, the designs with the converging channel, yielded lower values of R than Type I and II, as shown in Fig. 3a. The values of R for Type III and IV decreased by approximately 23% and 32% than those for Type I and II, respectively. The value of R in Type IV was reduced by about 15% compared to that of Type III. However, the value of R for Type II was slightly smaller than that for Type I. The results indicated that the design of the converging channels could significantly reduce the values of R , therefore, the efficiency of the extraction of cell-free plasma from whole blood could be enhanced. The existence of bending channels could improve the efficiency of the extraction of cell-free

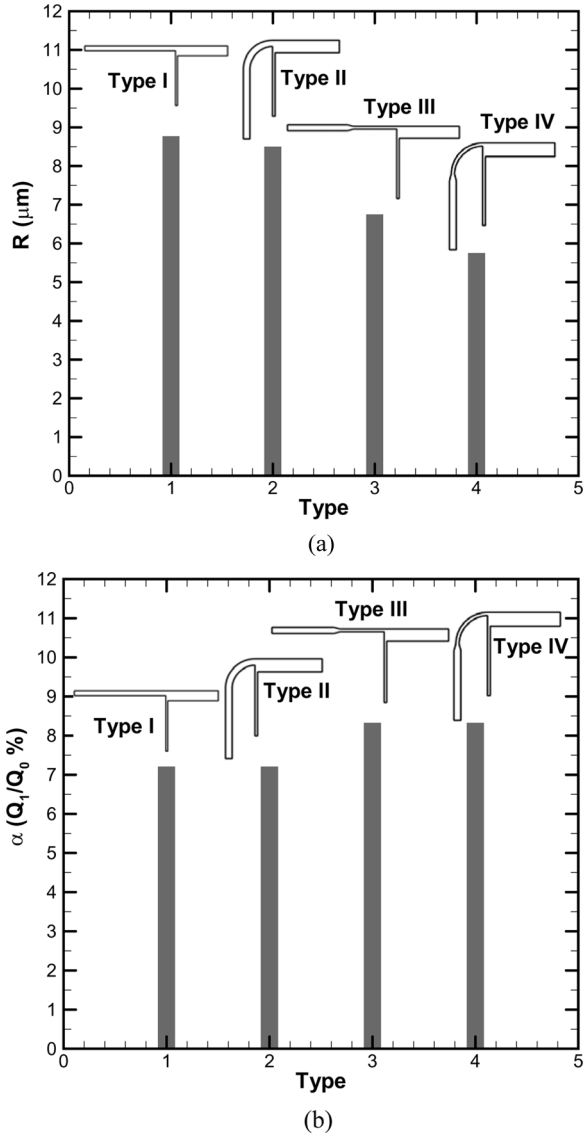


FIG. 3. (a) The minimum radius (R) of particles which can be excluded from the side channel and (b) fraction of the volumetric flowrate (α) for the four types of microchannels at a Reynolds number of 5.

plasma only for the designs with converging channels. The fractions of the volumetric flowrate (α) for the different designs depicted in Fig. 3b indicated that the values of α for Type III and IV were higher than those for Type I and II. Only designs with converging channels could improve the volumetric fraction of the extraction of cell-free plasma, according to the results in Fig. 3b. Based on the numerical simulations, Type IV was the optimum design among the layouts proposed in this work.

The previous results showed that the design of converging channels in Type III and IV could significantly enhance the efficiency of the extraction of cell-free plasma from whole blood. The values of R and α for type III and IV, with different Reynolds number (Re), were depicted in

Fig. 4. The values of R and α decreased as Re increased for both Type III and IV. The critical value of R was set as $1 \mu\text{m}$, due to the radius of platelets, which are the smallest cell in whole blood samples. When Re equals approximately 20, the critical value of R is achieved in Type IV, and α equals 8.4; however, Re had to be larger than 80 in Type III, and α was less than 5 in that case. Therefore, Type IV could separate smaller cells than the other types for the same Reynolds number (when Re is less than 85), as depicted in Fig. 4a. Moreover, the values of α for Type IV were larger than those for Type III when Re was higher than 40, and the differentials increased with increasing Re , as shown in Fig. 4b. The pressure fields of Type III and IV

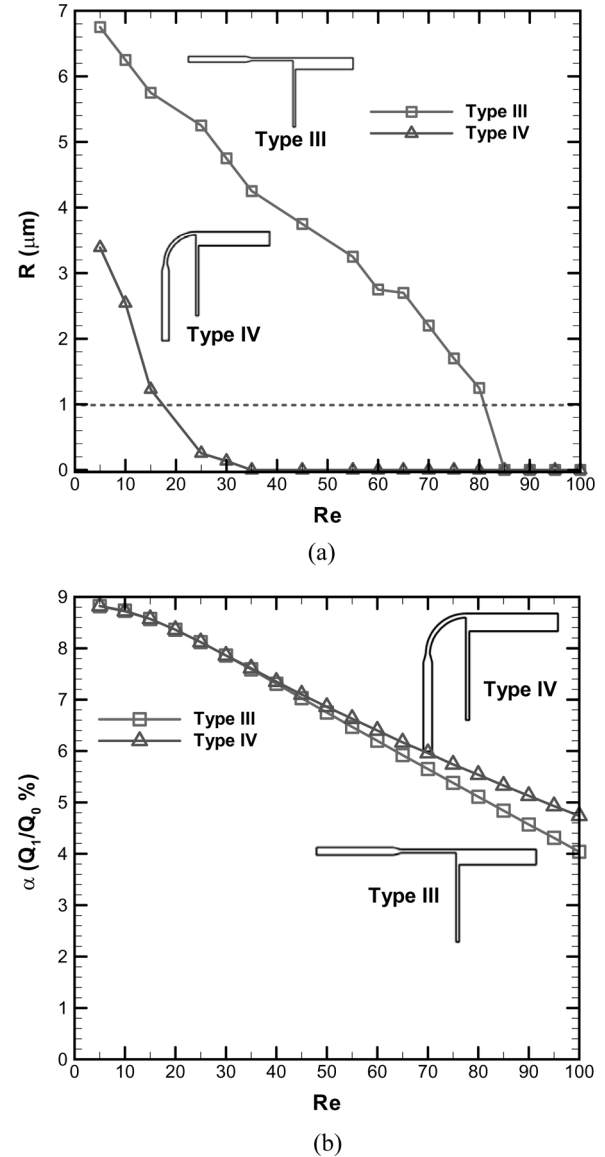


FIG. 4. The values of (a) R and (b) α for Type III and IV with different Reynolds numbers.

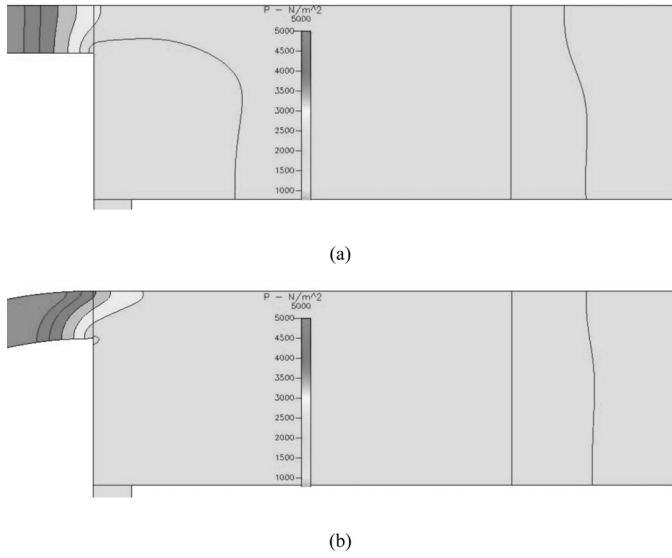


FIG. 5. The pressure field in the microchannel of (a) Type III and (b) Type IV when Re equals 90.

at Re equals 90, shown in Fig. 5, indicated that the pressure drop between the branch point and plasma outlet in Type IV, with the bent microchannel, was larger than that in Type III. This could explain why the values of α in

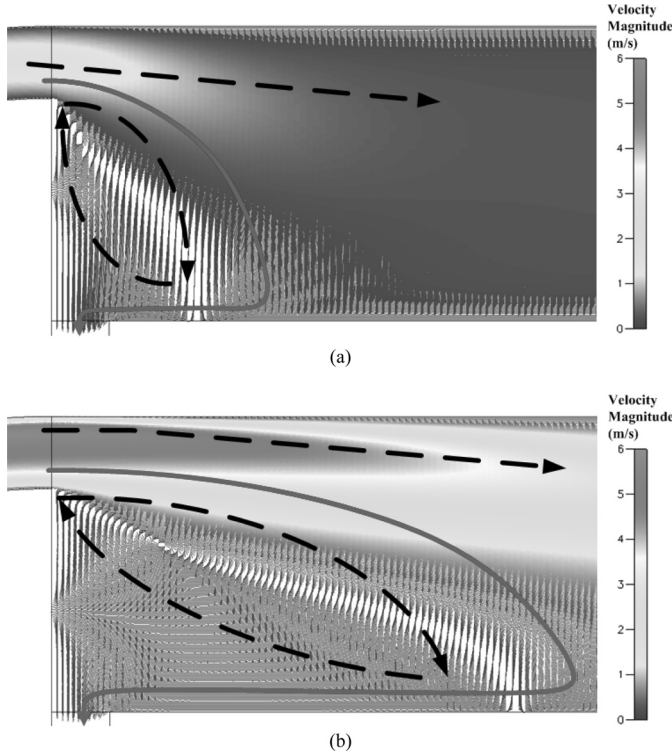


FIG. 6. The vector of the flow field for the Type IV microchannel with a Reynolds number of (a) 25 and (b) 100.

Type IV were larger than those in type III, for Re larger than 50. Figure 6 showed the vectors of the flow field of Re equals 25 and 100 in Type IV, respectively. When Re equals 100, the recirculation region enlarged more than when Re equals 25; thus, the flowrate distributed into the side channel decreased, and the volumetric fraction of the extraction of cell-free plasma was reduced. However, the increase of Reynolds number also reduced the possibility of particles entering the side channel. The simulated results revealed that the design of Type IV performed with the best efficiency of cell separation and plasma extraction. When Re equals approximately 20, the value of R could be less than the critical value, and a higher volumetric

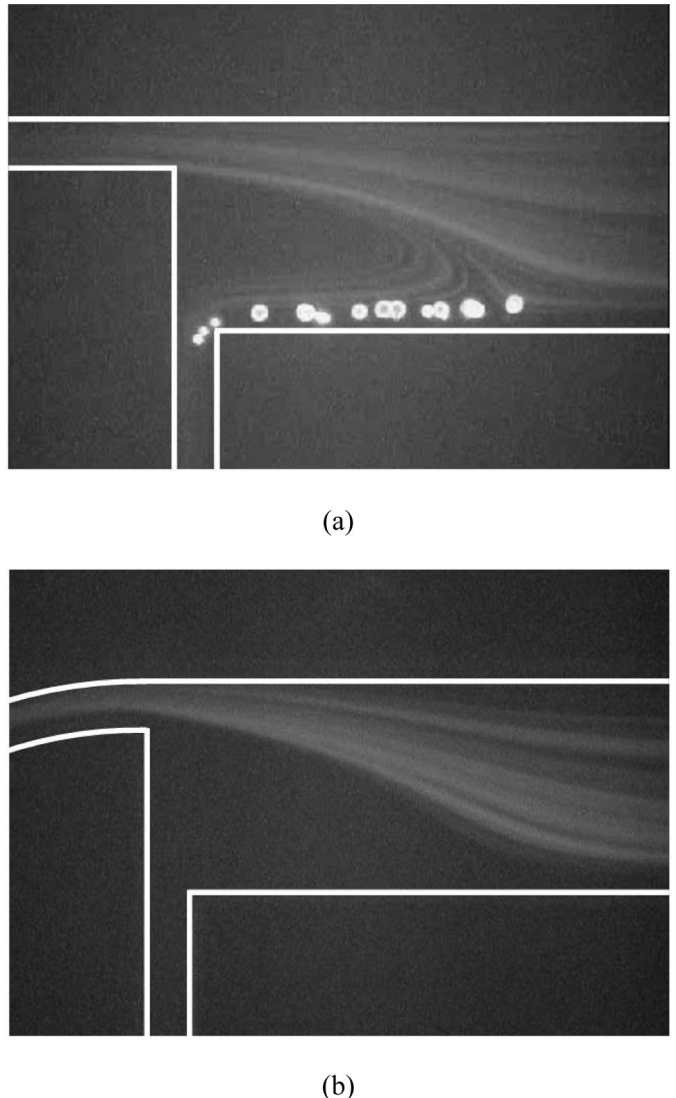


FIG. 7. The snapshots of particle trace images in the microchannels of (a) Type III and (b) Type IV when Re of the inlet flowrate equals 50 (the radius of fluorescent particles is $2.5 \mu\text{m}$).

fraction of extraction flowrate, which was about 8.4%, was simultaneously achieved.

The preliminary experiments were implemented to demonstrate the feasibility of the microfluidic chips for the plasma extraction. The microfluidic devices of Type III and IV were fabricated in-house, using standard photolithography techniques. The mold master was fabricated by spinning SU8-50 (MicroChem Corp. Newton, MA) on the silicon wafer to define the microchannels. The polydimethylsiloxane (PDMS) prepolymer mixture (Sylgard-184 Silicone Elastomer Kit, Dow Corning, Midland, MI) was poured and cured on the mold master to replicate the patterned structures. After peeling off the PDMS replica, the inlet and outlet ports were made by a puncher. It was bonded with the glass substrate after treatment of the oxygen plasma in the O₂ plasma cleaner. The fluorescent particles with a radius of 2.5 μm were injected into the microchannels while the Reynolds number of the inlet flowrate equals 50. The snapshots of particle trace images in the microchannels of Type III and IV were illustrated in Fig. 7. The experimental results depicted clearly that long time exposure of the particle (2.5 μm) traces do not enter the side channel of Type IV; however, the particles could flow into the side channel of Type III. The fluorescent particles are excluded from side (plasma outlet) channel of Type IV successfully. According to the numerical prediction in Fig. 4a, the particles with 2.5 μm in radius could be excluded from the side channel of Type IV, rather than that of Type III. The experimental results agreed with the numerical predictions well in the present study.

CONCLUSIONS

The usage of disposable microfluidic chips is attractive because of Point-of-Care (POC) applications. The present study involved the design of microfluidic chips with different microchannel structures, utilizing backward facing step geometry and centrifugal force to extract the cell-free plasma from whole blood samples at the branch of a microchannel for further assay, avoiding the influence of blood cells. Three-dimensional simulations were numerically performed to analyze the effects of inlet velocity and the structures of the microchannel on the flow field and back-flow in the microchannel, as well as the efficiency of separation and volumetric fraction of flowrate of plasma extraction. The minimum radius (R) of particles that can be excluded from the side channel, and the fraction of the volumetric flowrate (α), were obtained to evaluate the efficiency of plasma extraction. The goal of the optimum design is to achieve the lowest value of R and highest value of α . The design of converging channels could significantly reduce the values of R and enlarged the value of α . Type IV, with both converging and bending channels, was the best design among the four layouts proposed in this work.

The value of R obtained could be less than the critical value (set as 1 μm because of the radius of platelets) and the volumetric fraction of extraction flowrate was approximately 8.4%, for a Re of about 20. The preliminary experiments indicated the fluorescent particles with 2.5 μm in radius are excluded from plasma outlet channel of Type IV successfully, when the Reynolds number of the inlet flowrate equals 50.

ACKNOWLEDGEMENTS

The authors would like to thank the National Science Council of the Republic of China for its financial support of this research under contract No. NSC-96-2221-E-194-025-MY2 and the National Center for High-performance Computing for computer time and facilities.

REFERENCES

1. Toner, M.; Irimia, D. (2005) Blood-on-a-chip. *Annu. Rev. Biomed. Eng.*, 7: 77.
2. Fung, Y.C. (1993) *Biomechanics: Mechanical Properties of Living Tissues*; Springer-Verlag: New York.
3. Lüderitz, B.; Naumann d' Alnoncourt, C.; Steinbeck, G. (1976) Effects of free fatty acids on electrophysiological properties of ventricular myocardium. *Int. J. Mol. Med.*, 54 (7): 309.
4. Siami, G.A.; Siami, F.S. (2001) Membrane plasmapheresis in the united states: A review over the last 20 years. *Ther. Apher.*, 5 (4): 315.
5. Tüdös, A.J.; Besselink, G.A.J.; Schasfoort, R.B.M. (2001) Trends in miniaturized total analysis systems for point-of-care testing in clinical chemistry. *Lab Chip*, 1: 83.
6. Verpoorte, E. (2002) Microfluidic chips for clinical and forensic analysis. *Electrophoresis*, 23: 677.
7. Andersson, H.; van der Wijngaart, W.; Enoksson, P.; Stemme, G. (2000) Micromachined flow-through filter-chamber for chemical reactions on beads. *Sens. Actuator B-Chem.*, 67: 203.
8. He, B.; Tan, L.; Regnier, F. (1999) Microfabricated Filters for Microfluidic Analytical Systems. *Anal. Chem.*, 71: 1464.
9. Wilding, P.; Pfahler, J.; Bau, H.H.; Zemel, J.N.; Kricka, L.J. (1994) Manipulation and flow of biological fluids in straight channels micromachined in silicon. *Clin. Chem.*, 40: 43.
10. Lin, L.; Guthrie, J.T. (2000) Preparation and characterisation of novel, blood-plasma-separation membranes for use in biosensors. *J. Membr. Sci.*, 173: 73.
11. Yuen, P.K.; Kricka, L.J.; Fortina, P.; Panaro, N.J.; Sakazume, T.; Wilding, P. (2001) Microchip module for blood sample preparation and nucleic acid amplification reactions. *Genome Res.*, 11: 405.
12. Crowley, T.A.; Pizziconi, V. (2005) Isolation of plasma from whole blood using planar microfilters for lab-on-a-chip applications. *Lab Chip*, 5: 922.
13. Broyles, B.S.; Jacobson, S.C.; Ramsey, J.M. (2003) Sample filtration, concentration, and separation integrated on microfluidic devices. *Anal. Chem.*, 75: 2761.
14. Moorthy, J.; Beebe, D.J. (2003) In situ fabricated porous filters for Microsystems. *Lab Chip*, 3: 62.
15. Thorslund, S.; Klett, O.; Nikolajeff, F.; Markides, K.; Bergquist, J. (2006) A hybrid poly(dimethylsiloxane) microsystem for on-chip whole blood filtration optimized for steroid screening. *Biomed. Microdevices*, 8: 73.
16. VanDelinder, V.; Groisman, A. (2006) Separation of plasma from whole human blood in a continuous cross-flow in a molded microfluidic device. *Anal. Chem.*, 78 (11): 3765.

17. Jäggi, R.D.; Sandoz, R.; Effenhauser, C.S. (2007) Microfluidic depletion of red blood cells from whole blood in high-aspect-ratio microchannels. *Microfluid Nanofluid*, 3: 47.
18. Fan, R.; Vermesh, O.; Srivastava, A.; Yen, B.K.H.; Qin, L.; Ahmad, H.; Kwong, G.A.; Liu, C.-C.; Gould, J.; Hood, L.; Heath, J.R. (2008) Integrated barcode chips for rapid, multiplexed analysis of proteins in microliter quantities of blood. *Nat. Biotechnol.*, 26 (12): 1373.
19. Tachi, T.; Kaji, N.; Tokeshi, M.; Baba, Y. (2009) Simultaneous separation, metering, and dilution of plasma from human whole blood in a microfluidic System. *Anal. Chem.*, 81: 3194.
20. Duffy, D.C.; Gillis, H.L.; Lin, J.; Sheppard, Jr., N. F.; Kellogg, G.J. (1999) Microfabricated centrifugal microfluidic systems: Characterization and multiple enzymatic assays. *Anal. Chem.*, 71: 4669.
21. Madou, M.J.; Lee, L.J.; Daunert, S.; Lai, S.; Shih, C.H. (2001) Design and fabrication of CD-like microfluidic platforms for diagnostics: Microfluidic functions. *Biomed. Microdevices*, 3: 245.
22. Lai, S.; Wang, S.; Luo, J.; Lee, L.J.; Yang, S.T.; Madou, M.J. (2004) Design of a compact disk-like microfluidic platform for enzyme-linked immunosorbent assay. *Anal. Chem.*, 76: 1832.
23. Steigert, J.; Brenner, T.; Grumann, M.; Rieger, L.; Zengerle, R.; Ducrée, J. (2006) Design and fabrication of a centrifugally driven microfluidic disk for fully integrated metabolic assays on whole blood. In: *Proceedings of the 19th IEEE International Conference on Micro Electro Mechanical Systems (MEMS 2006)*, Istanbul, Turkey.
24. Cho, Y.-K.; Lee, J.-G.; Park, J.-M.; Lee, B.-S.; Lee, Y.; Ko, C. (2007) One-step pathogen specific DNA extraction from whole blood on a centrifugal microfluidic device. *Lab Chip*, 7: 565.
25. Yang, S.; Ündar, A.; Zahn, J.D. (2006) A microfluidic device for continuous, real time blood plasma separation. *Lab Chip*, 6: 871.
26. Blattert, C.; Jurischka, R.; Tahhan, I.; Schoth, A.; Kerth, P.; Menz, W. (2004) Separation of blood in microchannel bends. In: *Proceedings of the 26th Annual International Conference of the IEEE EMBS*, San Francisco, CA, U.S.A..
27. Park, J.; Cho, K.; Chung, C.; Han, D.-C.; Chang, J.K. (2005) Continuous plasma separation from whole blood using microchannel geometry. In: *Proceedings of the 3rd Annual International IEEE EMBS Special Topic Conference on Microtechnologies in Medicine and Biology*, Kahuku, Oahu, Hawaii.
28. Svanes, K.; Zweifach, B.W. (1968) Variations in small blood vessel hematocrits produced in hypothermic rats by micro-occlusion. *Microvasc. Res.*, 1 (2): 210.
29. Fung, Y. C. (1973) Stochastic flow in capillary blood vessels. *Microvasc. Res.*, 5 (1): 34.
30. Yamada, M.; Seki, M. (2006) Microfluidic particle sorter employing flow splitting and recombining. *Anal. Chem.*, 78: 1357.
31. Nie, Z.; Cui, F.; Tzeng, Y.-K.; Chang, H.-C.; Chu, M.; Lin, H.-C.; Chen, C.-H.; Lin, H.-H.; Yu, A.L. (2007) High-speed mass analysis of whole erythrocytes by charge-detection quadrupole ion trap mass spectrometry. *Anal. Chem.*, 79: 7401.